Research Article

Cancer Prevention Research

Using Digital Pathology to Understand Epithelial Characteristics of Benign Breast Disease among Women Undergoing Diagnostic Image-Guided Breast Biopsy

Maeve Mullooly[1], Samantha Puvanesarajah[2], Shaoqi Fan[3], Ruth M. Pfeiffer[3], Linnea T. Olsson[4], Manila Hada[3], Erin L. Kirk[4], Pamela M. Vacek[5], Donald L. Weaver[5], John Shepherd[6], Amir Mahmoudzadeh[7], Jeff Wang[8], Serghei Malkov[7], Jason M. Johnson[9], Stephen M. Hewitt[10], Sally D. Herschorn[5], Mark E. Sherman[11], Melissa A. Troester[4], and Gretchen L. Gierach[3]

Abstract

Delayed terminal duct lobular unit (TDLU) involution is associated with elevated mammographic breast density (MD). Both are independent breast cancer risk factors among women with benign breast disease (BBD). Prior digital analyses of normal breast tissues revealed that epithelial nuclear density (END) and TDLU involution are inversely correlated. Accordingly, we examined associations of END, TDLU involution, and MD in BBD clinical biopsies. This study included digitized images of 262 representative image-guided hematoxylin and eosin–stained biopsies from 224 women diagnosed with BBD, enrolled within the cross-sectional BREAST-Stamp project that were visually assessed for TDLU involution (TDLU count/100 mm^2, median TDLU span and median acini count per TDLU). A digital algorithm estimated nuclei count per unit epithelial area, or END. Single X-ray absorptiometry of prebiopsy ipsilateral craniocaudal digital mammograms measured global and localized MD surrounding the biopsy region. Adjusted ordinal logistic regression models assessed relationships between tertiles of TDLU and END measures. Analysis of covariance examined mean differences in MD across END tertiles. TDLU measures were positively associated with increasing END tertiles [TDLU count/100 mm^2, OR_{T3vsT1}: 3.42, 95% confidence interval (CI), 1.87–6.28; acini count/$TDLU_{T3vsT1}$, OR: 2.40, 95% CI, 1.39–4.15]. END was significantly associated with localized, but not, global MD. Relationships were most apparent among patients with nonproliferative BBD. These findings suggest that quantitative END reflects different but complementary information to the histologic information captured by visual TDLU and radiologic MD measures and merits continued evaluation in assessing cellularity of breast parenchyma to understand the etiology of BBD.

[1]Division of Population Health Science, Royal College of Surgeons in Ireland, Dublin, Ireland. [2]Behavioral and Epidemiology Research Program, American Cancer Society, Atlanta, Georgia. [3]Division of Cancer Epidemiology and Genetics, National Cancer Institute, Bethesda, Maryland. [4]Department of Epidemiology, The University of North Carolina at Chapel Hill, Chapel Hill, North Carolina. [5]The University of Vermont and The University of Vermont Cancer Center, Burlington, Vermont. [6]University of Hawaii Cancer Center, Honolulu, Hawaii. [7]University of California, San Francisco, San Francisco, California. [8]Department of Radiation Medicine, Hokkaido University Graduate School of Medicine, Sapporo, Hokkaido, Japan. [9]The University of Texas MD Anderson Cancer Center, Houston, Texas. [10]Center for Cancer Research, National Cancer Institute, Bethesda, Maryland. [11]Mayo Clinic, Jacksonville, Florida.

Note: Supplementary data for this article are available at Cancer Prevention Research Online (http://cancerprevres.aacrjournals.org/).

M. Mullooly and S. Puvanesarajah contributed equally to this article.

M. Mullooly and S. Puvanesarajah are the co-first authors of this article.

M.E. Sherman, M.A. Troester, and G.L. Gierach are the co-senior authors of this article.

Corresponding Author: Maeve Mullooly, Division of Population Health Sciences, Royal College of Surgeons in Ireland, Beaux Lane House, Mercer Street Lower, Dublin 2, Ireland. Phone: +353-1-402-8661; Fax: +353-1-402-2764; E-mail: maevemullooly@rcsi.ie

Cancer Prev Res 2019;12:861–70

doi: 10.1158/1940-6207.CAPR-19-0120

Introduction

Normal breast tissue is composed of varying amounts of fibroglandular (i.e., stromal and epithelial tissues) and adipose tissues. Elevated mammographic breast density (MD), which reflects a higher percentage of fibroglandular tissue within the breast parenchyma, is a strong breast cancer risk factor (1, 2). Women with the highest levels of MD have 4- to 6-fold increased risk of developing breast cancer compared with women with the lowest level of MD (2). It has been hypothesized that increased numbers of at-risk epithelial cells represent a probable mechanism influencing this risk association; however, quantitative metrics for at-risk epithelial cells are lacking.

One approach to quantifying at-risk epithelium has focused on assessing terminal duct lobular units (TDLUs), the primary epithelial structures that produce most breast cancer precursors (3). Among women who have undergone a biopsy demonstrating benign breast disease (BBD), delayed age-dependent TDLU involution has been associated with increased breast cancer risk, independent of BBD severity and MD (4). To date, most studies have examined TDLU involution using visual assessment, methods that are labor intensive (5). Although standardized, these measures are semiquantitative rather than quantitative and require intact complete TDLU structures (6). Digital histologic approaches that quantitatively and objectively measure breast tissue morphometry may provide a high-throughput method suitable for epidemiologic applications to further our understanding of breast cancer etiology. Digital measures can also be performed even when TDLU structures are incompletely captured on a slide, decreasing potential missing assessments in histologic analyses.

A prior study of normal breast tissues that applied digital histologic assessment revealed that the digitally quantified measure of epithelial cells termed "epithelial nuclear density" (END) decreased with older age (7) and raised the possibility that the quantification of nuclei may represent a high-throughput method of TDLU involution assessment. Furthermore, among normal breast tissues, higher END was associated with elevated MD assessed using the visual Breast Imaging Reporting and Data Systems (BI-RADS) density scale (8). In this study, we expand these prior findings by applying digital assessment to an independent population of BBD biopsies of nonproliferative and proliferative diagnoses. We also examined relationships of END with visual measures of TDLU involution as well as with quantitatively assessed global and localized MD measures, among women undergoing a diagnostic breast biopsy.

Methods

Study population

This study included 224 women, who participated in the National Cancer Institute's (NCI) Breast Radiology Evaluation and Study of Tissues (BREAST)-Stamp Project, a cross-sectional molecular epidemiology study of MD. Participants were women referred for diagnostic image-guided breast biopsy following an abnormal mammogram. Women ($n = 465$) were consented between 2007 and 2010 at the University of Vermont College of Medicine as described elsewhere (9–11). Eligible women were 40 to 65 years of age, did not have breast implants, did not have a previous breast cancer diagnosis, and were not administered treatment for any cancer or chemoprevention. Detailed demographic and risk factor data were collected on all enrolled participants through a questionnaire that was administered routinely at the time of mammogram and following a subsequent interview that was completed by the study research coordinator (9–11). This study was conducted in accordance with recognized ethnical guidelines (U.S. Common Rule). This study was performed following approval of the study protocol by the institutional review boards at the NCI and The University of Vermont. Informed consent was provided to the study investigators from all study participants prior to enrollment in the study.

Women underwent stereotactic-guided or ultrasound-guided biopsy for clinical management and pathologic diagnosis for routine care. This current study was restricted to women diagnosed with BBD and thus included 224 women with 262 BBD biopsies. Among these women, 190 women had one biopsy, 30 women had two biopsies, and 4 women had three biopsies. Women were not included in this study if they did not undergo a breast biopsy, if biopsy tissue was not available for hematoxylin and eosin (H&E) assessment, or if breast density measurements were not available. In this analysis, BBD subtype refers to diagnoses classified as nonproliferative (34.4%) versus proliferative, which included proliferative BBD without atypia (54.6%) and proliferative BBD with atypia (11.1%). Mean (SD) ages at diagnosis with nonproliferative and proliferative BBD were 49.6 (6.7) and 50.7 (6.5) years, respectively.

END assessment

A representative slide from the diagnostic target biopsy was sectioned, processed, and stained with H&E for research purposes at the same time that the biopsy was processed for clinical diagnosis. This representative H&E section was scanned and digitized at 20× using Aperio, Scanscope and prepared for digital review and annotation using Digital Image Hub software (SlidePath/Leica). For the quantitative assessment of END shown in Fig. 1A–C, an image-based algorithm developed through Aperio's Genie Classifier was applied to the whole slide image to define epithelium, stroma, and adipose tissue composition. Prior analyses confirmed strong agreement (≥95%) between this automated assessment and pathologist semiquantitative visual review (7, 8). Assessment of END was restricted to H&E slides where the proportion of tissue stroma on the

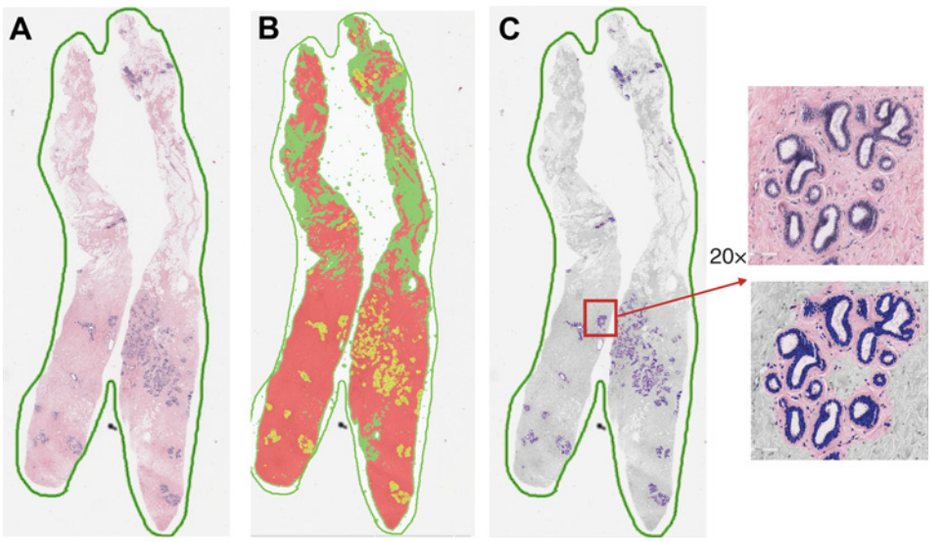

Figure 1.
A, Representative image of a BREAST-Stamp image-guided breast biopsy H&E. **B,** Application of the Genie Classifier (Aperio) to the whole slide image to define epithelium, stroma, and adipose tissue composition. Yellow, epithelium; red, stroma; and green, fat. **C,** Application of the END algorithm to the image to estimate nuclei count per unit epithelial area.

slide was $\geq$10%. The number of nuclei per unit area in the epithelium (END) was estimated using a validated nuclear detection Genie algorithm (7, 8).

TDLU involution histologic assessment

Three standardized measures of TDLU involution were visually assessed by the study pathologist (M.E. Sherman) in background normal tissue of the BBD biopsies, as previously outlined (6). Briefly, using the digitized H&E-stained sections, TDLU number was expressed as a density (TDLU count/100 mm^2). Tissue area was determined using the Lasso function on Digital Image Hub software. For up to 10 TDLUs per image, the TDLU diameter (microns; TDLU span) and the number of acini per TDLU categorically were estimated (12, 13). Median values for each patient were used as summary measures of TDLU span and TDLU acini count.

Assessment of global and localized MD

Global and localized MD measures were assessed at the University of California, San Francisco as previously outlined (10, 11), using prebiopsy craniocaudal digital raw mammograms of the ipsilateral breast. First, global MD was estimated using single X-ray absorptiometry (SXA) as percent fibroglandular volume (FGV), in which an SXA breast density phantom was affixed to the compression paddle of the mammography machine, included in the X-ray field, and served as a reference standard to estimate MD volumetrically (10). Second, for localized MD measurements, the biopsy location and radius were identified on the prebiopsy mammogram by the radiologist (11). SXA was used to estimate perilesional (localized) FGV centered at the biopsy site that measured twice the size of the biopsy lesion but excluding the biopsy target. Reproducibility statistics for the assessments of localized MD measures showed strong repeat reliability, with all interclass correlation coefficients >0.70 (10).

Statistical analysis

To visualize the relationship between averaged END and age at mammogram, the SAS procedure PROC LOESS that plotted a locally weighted smoothing (LOESS) curve was used. Descriptive relationships between breast cancer risk factors and END in tertiles were determined using χ^2 and Fisher exact tests. Adjusted ordinal logistic regression models were used to examine relationships between tertiles of TDLU with END measures. To determine whether these relationships varied by BBD diagnosis (nonproliferative or proliferative), we tested for interactions between TDLU/END measures and BBD diagnosis. Analysis of covariance (ANCOVA) was used to examine mean differences in MD across tertiles of END. Associations between TDLU/MD measures and END were visually examined using scatterplots. To better approximate normal distributions, MD measures were square root transformed for the ANCOVA analysis. For ease of interpretation, ANCOVA least square means and standard errors were subsequently back-transformed and corresponding confidence intervals (CI) were calculated for the MD measures for the original scale. Analyses are presented unadjusted and adjusted for both age and body mass index (BMI) as categorical variables, factors that are both strongly correlated with breast density. All analyses were conducted at the biopsy target level using a generalized estimating equation approach that accounts for multiple biopsies from the same woman in the variance computation (14). Analyses were conducted for the full study population and stratified by BBD diagnosis and menopausal status. Probability values of <0.05 were considered statistically significant. All tests of statistical significance were two-tailed. Analyses were conducted using the

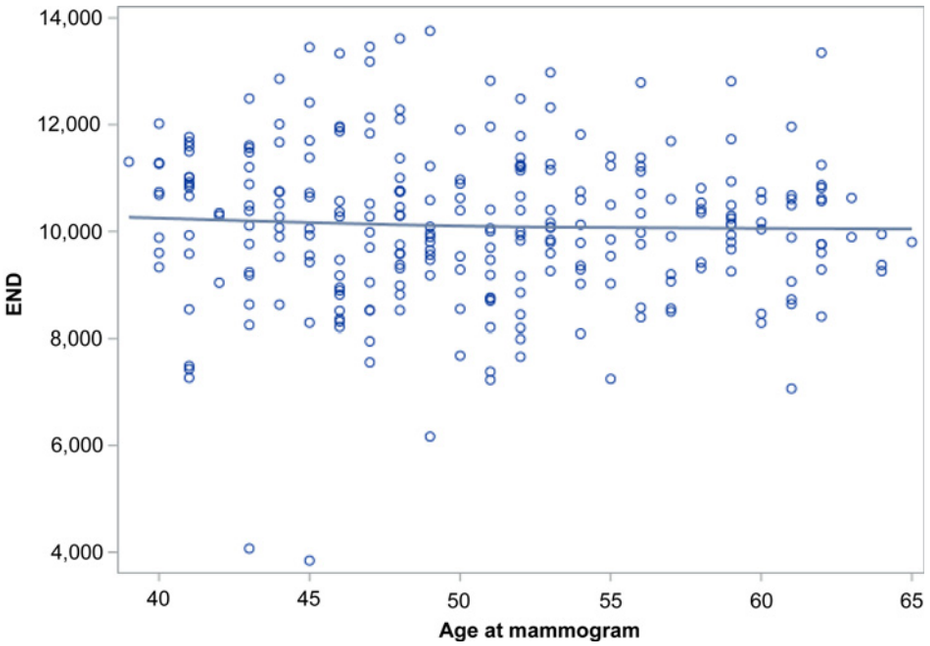

Figure 2.
Representative LOESS curve showing relationships between END and age at mammogram among women with benign breast disease, The BREAST-Stamp Project ($N = 224$ women; 262 biopsy targets).

PROC GENMOD function within the SAS statistical software (SAS Institute Inc.).

Results

Distribution of END measures among study participants

We first examined the distribution of END measures and how END measures related to patient characteristics. As shown in the LOESS curve in Fig. 2, which was plotted to visualize the relationships, a mostly flat relationship between END and age at mammogram was observed (Fig. 2).

When END was categorized into tertiles, although we observed a statistically significant inverse association between END and age at mammogram ($P = 0.041$), these associations were largely driven by differences within the highest tertile. Similar patterns of association were observed for associations between END and menopausal status ($P = 0.047$), with postmenopausal women having lower END as compared with premenopausal women, particularly for the highest END tertile (Supplementary Table S1). END measures were largely unrelated to the other patient characteristics examined (Supplementary Table S1).

Relationships between measures of TDLU involution and END measures

Relationships between tertiles of TDLU measures and tertiles of END are shown in Table 1. In ordinal logistic models for the overall population adjusted for age and BMI, significant positive associations were observed for the highest versus lowest tertiles of TDLU count/100 mm^2 (OR_{T3vsT1}: 3.42, 95% CI, 1.87–6.28) and acini count/TDLU (OR_{T3vsT1}: 2.40, 95% CI, 1.39–4.15) with END. No statistically significant relationships were observed for TDLU span following age and BMI adjustment. Corresponding scatterplots showing relationships between TDLU measures and END are shown in Supplementary Fig. S1A–S1C.

When analyses were stratified according to BBD subtype, similar associations for TDLU count and END were observed for those with proliferative and nonproliferative BBD diagnoses. Stronger associations for both TDLU span ($OR_{T3vsT1,\ Nonproliferative}$: 3.41, 95% CI, 1.07–10.92; $OR_{T3vsT1,\ Proliferative}$: 1.34, 95% CI, 0.65–2.79) and acini count/TDLU ($OR_{T3vsT1,\ Nonproliferative}$: 3.90, 95% CI, 1.41–10.80; $OR_{T3vsT1,\ Proliferative}$: 1.92, 95% CI, 1.02–3.61) with END were found for women with nonproliferative BBD, whereas the associations were attenuated among women with proliferative disease (Table 1). However, tests for interaction showed that these associations (OR and 95% CI) were not significantly different by BBD status ($P_{Interaction} > 0.2$). In analyses stratified by menopausal status, associations between TDLU count and END were stronger among premenopausal than postmenopausal women (Supplementary Table S2A). Similar patterns and strengths of associations were also observed when the analysis was restricted to parous women as compared with the main findings, though the strength of the associations was attenuated with the smaller sample size (Supplementary Table S2A).

Relationships between END measures and global and localized MD

Whereas TDLU measures were significantly associated with MD as previously described in this study

Table 1. Associations between TDLU measures and END tertiles among women with benign breast disease, overall, and by biopsy diagnosis subtypes, The BREAST-Stamp Project ($N = 224$ women; 262 biopsy targets)

	END														
	Overall, $n = 262$					Benign nonproliferative disease, $n = 90$					Benign proliferative disease, $n = 172$				
TDLU measures	T1 $N = 89$	T2 $N = 87$	T3 $N = 86$	Unadjusted OR (95% CI)[a]	Adjusted for age and BMI OR (95% CI)[a]	TDLU measures	T1 $N = 31$	T2 $N = 29$	T3 $N = 30$	Unadjusted OR (95% CI)[a]	Adjusted for age and BMI OR (95% CI)[a]	TDLU measures	T1 $N = 59$	T2 $N = 56$	T3 $N = 57$	Unadjusted OR (95% CI)[a]	Adjusted for age and BMI OR (95% CI)[a]
TDLU count/100 mm^2						**TDLU count/100 mm^2**						**TDLU count/100 mm^2**					
T1 (0–6.05)	40	29	20	Ref		T1 (0–2.0)	13	9	9	Ref	Ref	T1 (0–9.5)	26	19	14	Ref	Ref
T2 (6.06–24.8)	30	36	21	1.35 (0.79–2.30)	1.32 (0.77–2.27)	T2 (2.1–14.5)	11	12	6	0.94 (0.39–2.23)	1.04 (0.42–2.60)	T2 (9.6–31.3)	23	19	14	1.11 (0.56–2.20)	1.01 (0.50–2.02)
T3 (24.9–200)	19	22	45	**3.55 (2.97–6.40)**	**3.42 (1.87–6.28)**	T3 (14.6–200)	7	8	15	2.55 (0.98–6.62)	**3.11 (1.15–8.42)**	T3 (31.4–173)	10	18	29	**3.49 (1.73–7.06)**	**3.07 (1.46–6.45)**
P_{trend}				**<0.0001**	**0.0002**	P_{trend}				0.07	**0.03**	P_{trend}				**0.0007**	**0.0045**
P^b	**<0.0001**					P^b	0.14					P^b	**0.004**				
Weighted kappa	**0.23 (0.13–0.33)**					Weighted kappa	**0.18 (0.01–0.35)**					Weighted kappa	**0.21 (0.09–0.32)**				
Median TDLU span, μ						**Median TDLU span, μ**						**Median TDLU span, μ**					
T1 (115–221.0)	28	27	19	Ref	Ref	T1 (115–204.0)	10	6	6	Ref	Ref	T1 (125–227.0)	21	21	11	Ref	Ref
T2 (221.1–284.5)	26	22	24	1.24 (0.66–2.30)	1.18 (0.63–2.20)	T2 (204.1–258.5)	6	9	6	1.58 (0.50–5.03)	1.60 (0.50–5.15)	T2 (227.1–286.0)	17	13	21	1.83 (0.86–3.93)	1.62 (0.75–3.52)
T3 (284.6–628)	16	28	29	**1.97 (1.09–3.57)**	1.64 (0.88–3.05)	T3 (258.6–628)	3	8	10	**3.44 (1.05–11.27)**	**3.41 (1.07–10.92)**	T3 (286.1–578)	14	19	18	1.80 (0.91–3.57)	1.34 (0.65–2.79)
P_{trend}				**0.02**	0.11	P_{trend}				**0.048**	**0.04**	P_{trend}				0.08	0.41
P^b	0.17					P^b	0.21					P^b	0.17				
Weighted kappa	0.09 (−0.01 to 0.2)[c]					Weighted kappa	**0.22 (0.03–0.42)**[c]					Weighted kappa	0.07 (−0.05 to 0.19)[c]				
No TDLUs observed	19	10	14			No TDLUs observed	12	6	8			No TDLUs observed	7	3	7		
Median acini count per TDLU						**Median acini count per TDLU**						**Median acini count per TDLU**					
1–10	48	46	33	Ref	Ref	1–10	16	12	9	Ref	Ref	1–10	32	34	24	Ref	Ref
>10–15	10	6	7	0.95 (0.40–2.28)	0.91 (0.37–2.22)	>10–15	1	3	4	3.91 (0.92–16.71)	4.37 (0.95–20.05)	>10–15	10	1	4	0.38 (0.11–1.29)	0.31 (0.094–1.04)
≥16	12	25	32	**2.57 (1.49–4.42)**	**2.40 (1.39–4.15)**	≥16	2	8	9	**3.74 (1.32–10.59)**	**3.90 (1.41–10.80)**	≥16	10	18	22	**2.12 (1.14–3.94)**	**1.92 (1.02–3.61)**
P_{trend}				**0.001**	**0.003**	P_{trend}				**0.009**	**0.004**	P_{trend}				**0.03**	0.08
P^b	**0.01**					P^b	0.07					P^b	**0.006**				
Weighted kappa	**0.16 (0.06–0.26)**[c]					Weighted kappa	**0.24 (0.07–0.42)**[c]					Weighted kappa	0.10 (−0.02 to 0.22)[c]				
No TDLUs observed	19	10	14			No TDLUs observed	12	6	8			No TDLUs observed	7	3	7		

NOTE: P value less than 0.05 is shown in values in bold. The cutoffs of END tertiles among overall patients were as follows: T1: 3842–9598.0, T2: 9598.1–10674.0, T3: 10674.1–13757; the cutoffs of END tertiles among patients with nonproliferative breast disease were as follows: T1: 3842–9178.0, T2: 9178.1–10569.0, T3: 10569.1–13461; the cutoffs of END tertiles among patients with proliferative breast disease were as follows: T1: 4069–9751.0, T2: 9751.1–10749.0, T3: 10749.1–13757.

Abbreviations: BMI, body mass index; CI, confidence interval; END, epithelial nuclear density; OR, odds ratio; T, tertile; TDLU, terminal duct lobular unit.

[a]ORs and 95% CI estimates were calculated using ordinal logistic regression models. Multivariable models were adjusted for age and BMI as categorized trends. $P_{trend} < 0.05$ are presented in values in bold.

[b]P value is from χ^2 test.

[c]Weighted kappa test excluded biopsy targets with zero TDLU observed.

Table 2. Associations between END tertiles and MD measures among women with benign breast disease, overall and by biopsy diagnosis subtypes, The BREAST-Stamp Project ($N = 224$ women; 262 biopsy targets)

	Overall ($N = 262$)							
	Percent dense area		**Percent fibroglandular volume**		**Percent perilesional fibroglandular volume**		**Percent lesional fibroglandular volume**	
END tertiles	**Mean (95% CI)**	**Adjusted mean (95% CI)[a]**	**Mean (95% CI)**	**Adjusted mean (95% CI)[a]**	**Mean (95% CI)**	**Adjusted mean (95% CI)[a]**	**Mean (95% CI)**	**Adjusted mean (95% CI)[a]**
Tertile 1	26.1 (22.9–29.4)	27.0 (24.2–29.9)	36.9 (33.5–40.3)	38.2 (35.4–41.0)	40.3 (36.5–44.0)	41.4 (38.2–44.6)	43.6 (39.8–47.4)	44.7 (41.3–48.0)
Tertile 2	25.4 (23.0–28.3)	25.9 (23.4–28.3)	38.9 (35.9–41.8)	39.2 (36.9–41.5)	43.8 (40.3–47.3)	44.2 (41.2–47.2)	47.7 (44.2–51.2)	48.3 (45.3–51.2)
Tertile 3	29.3 (25.9–32.7)	27.8 (25.0–30.7)	42.7 (38.9–46.5)	40.9 (38.0–43.8)	50.7 (46.7–54.7)	48.9 (45.4–52.3)	53.5 (49.5–57.6)	51.7 (48.2–55.2)
P_{trend}	0.32	0.78	0.1	0.30	**0.007**	**0.02**	**0.01**	**0.03**
	Nonproliferative disease ($N = 90$)							
	Percent dense area		**Percent fibroglandular volume**		**Percent perilesional fibroglandular volume**		**Percent lesional fibroglandular volume**	
END tertiles	**Mean (95% CI)**	**Adjusted mean (95% CI)[a]**	**Mean (95% CI)**	**Adjusted mean (95% CI)[a]**	**Mean (95% CI)**	**Adjusted mean (95% CI)[a]**	**Mean (95% CI)**	**Adjusted mean (95% CI)[a]**
Tertile 1	24.7 (19.1–30.3)	23.9 (19.4–28.4)	33.5 (28.1–39.0)	32.5 (28.4–36.6)	37.7 (31.1–44.3)	36.7 (31.5–41.8)	41.2 (34.5–47.8)	40.1 (34.8–45.4)
Tertile 2	24.5 (20.0–29.1)	24.1 (20.1–28.1)	38.0 (33.3–42.5)	37.3 (33.3–41.3)	41.2 (35.2–47.1)	40.5 (35.4–45.6)	45.1 (39.0–51.2)	44.4 (39.1–49.7)
Tertile 3	26.8 (21.6–31.9)	28.0 (23.3–32.7)	38.8 (33.0–44.7)	40.6 (36.0–45.2)	44.0 (36.7–51.2)	45.8 (39.2–52.3)	47.4 (40.6–54.2)	49.2 (43.1–55.3)
P_{trend}	0.69	0.34	0.34	0.06	0.36	0.10	0.35	0.10
	Proliferative disease ($N = 172$)							
	Percent dense area		**Percent fibroglandular volume**		**Percent perilesional fibroglandular volume**		**Percent lesional fibroglandular volume**	
END tertiles	**Mean (95% CI)**	**Adjusted mean (95% CI)[a]**	**Mean (95% CI)**	**Adjusted mean (95% CI)[a]**	**Mean (95% CI)**	**Adjusted mean (95% CI)[a]**	**Mean (95% CI)**	**Adjusted mean (95% CI)[a]**
Tertile 1	28.5 (24.6–32.4)	30.3 (26.6–34.0)	39.1 (35.0–43.2)	41.6 (38.2–45.0)	43.1 (38.7–47.5)	45.2 (41.2–49.1)	46.1 (41.7–50.6)	48.2 (44.1–52.2)
Tertile 2	25.5 (21.8–29.1)	25.3 (22.7–27.8)	40.5 (36.5–44.6)	40.2 (37.5–42.9)	46.4 (42.1–50.7)	46.3 (43.2–49.5)	50.2 (45.9–54.6)	50.2 (47.0–53.5)
Tertile 3	29.6 (25.2–34.0)	27.8 (24.1–31.5)	43.3 (38.5–48.1)	41.0 (37.4–44.6)	51.5 (46.7–56.3)	49.3 (45.1–53.4)	54.4 (49.6–59.3)	52.2 (47.8–56.5)
P_{trend}	0.79	0.46	0.34	0.85	0.06	0.29	0.07	0.33

NOTE: $P_{trend} < 0.05$ are presented in values in bold. The cutoffs of END tertiles among overall patients were as follows: T1: 3842–9598.0, T2: 9598.1–10674.0, T3: 10674.1–13757; the cutoffs of END tertiles among patients with nonproliferative breast disease were as follows: T1: 3842–9178.0, T2: 9178.1–10569.0, T3: 10569.1–13461; the cutoffs of END tertiles among patients with proliferative breast disease were as follows: T1: 4069–9751.0, T2: 9751.1–10749.0, T3: 10749.1–13757.

Abbreviations: BMI, body mass index; CI, confidence interval; END, epithelial nuclear density.

[a]Models adjusted for age and BMI as categorical trends.

population (11), no statistically significant relationships were observed between END and global MD (percent dense area and percent FGV; Table 2). Corresponding scatterplots showing relationships between MD measures and END are shown in Supplementary Fig. S2A–S2C. In analyses stratified by BBD diagnosis, there was a suggestive positive association between END and global percent FGV among patients with nonproliferative ($P = 0.06$), but not proliferative ($P = 0.85$), BBD. In contrast, statistically significant trends for the positive associations of increasing localized percent perilesional and lesional MD were observed with increasing tertiles of END, adjusted for age and BMI, among the total BBD population. These findings were attenuated upon stratification by BBD diagnosis, though they were most apparent for those with nonproliferative BBD status (Table 2). Furthermore, in analyses stratified by menopausal status, the positive association between localized MD measures and END was observed only among premenopausal women (Supplementary Table S2B). Findings showing associations with absolute dense measures are shown in Supplementary Table S3. In general, absolute dense area and FGV decreased with increased END tertiles, with statistically significant trends observed only for absolute FGV.

***Post hoc* sensitivity analysis**

To investigate and aim to explain the observed differences in associations between END measures and TDLU measures according to BBD status, we conducted *post hoc* additional analyses. END assessments were repeated on segmented images derived from our pathologist's annotations of the background normal tissue areas on the H&E whole-slide image to restrict END assessment to the normal tissue areas, which were visually assessed for TDLU metrics by the study pathologist. In this sensitivity analysis, women with no apparent normal TDLUs were assigned an END measure of zero. Associations between segmented END regions and TDLU counts are shown in Supplementary Table S4. Despite a loss in precision due to small sample sizes within the tertiles, similar and stronger patterns of positive associations were observed for the relation of TDLU counts with the segmented END metric (OR_{T3vsT1}: 7.08, 95% CI, 3.77–13.29). Furthermore, these stronger positive trends were also observed among women with both benign nonproliferative and proliferative diseases (Supplementary Table S4).

Discussion

Understanding the at-risk epithelial tissue among women with an imaging detected mammographic abnormality may provide clues about precursor BBD lesions and their potential to progress to breast cancer. It has been hypothesized that increased numbers of at-risk epithelial cells may reflect a probable mechanism underlying the MD–breast cancer risk associations, and we sought an automated approach for quantifying epithelium to determine whether an automated measure (END) could be used as a surrogate for the labor-intensive visual assessment of TDLUs. Our findings demonstrate that digital approaches can be used to capture epithelial histologic information. We observed positive associations between visual TDLU and automated END assessments. Furthermore, we identified positive associations between END and measures of MD localized at the biopsy target. Simultaneously, we found that although these automated and visual breast epithelial metrics are correlated, they reflect different histologic features and quantitative scales and capture different architectural aspects of the tissue. These findings suggest that END reflects complementary information to the histologic information captured by TDLU measures and radiological MD measures but may not be used as a surrogate of each measure within the setting of BBD. However, END may be an acceptable surrogate of TDLU involution within "normal" breast tissue. Together this study merits continued evaluation in assessing cellularity of breast parenchyma to understand the etiology of BBD.

Prior reports using normal breast tissue showed that increasing age is associated with reduced END and stromal proportions within the breast, reflecting declining-related stromal components and increasing relative adipose tissue in conjunction with age-related MD decline (7). In this analysis, we did not observe strong associations between END and patient's age. However, the range of ages in our population was restricted to women undergoing screening mammography, ages 40 to 65 years, and shifted toward older ages relative to the previous studies. The stronger associations observed among premenopausal women suggest the potential utility of this tool in younger women where complete involution is less apparent. Our results also showed positive associations between END and localized MD, which support prior findings of stronger associations between TDLUs and localized MD within this study population (11). Therefore, these findings support these localized radiodense areas that were targeted for suspicious abnormality as regions of increased epithelial content.

Automated digital pathologic approaches using whole slide images are increasingly being developed and applied in the classification of breast tissue morphology (for review, see ref. 5). To date, two published studies have utilized the END algorithm applied in this study. Compared with that prior work (7, 8) our tissue specimens showed higher mean distributions of END measures (7, 8). This finding may be expected, given that our study included only women diagnosed with BBD after undergoing a biopsy following an abnormal mammogram, whereas women with specimens for previous studies were not selected for mammographic abnormalities (7). Thus, the study population and disease type are important factors to consider for the utility of the END imaging tool and for interpreting subsequent measures.

Additional factors that should be considered when interpreting END findings include variability in the tissue specimens and possible technical differences in slide preparation or image analysis. For example, Sandhu and colleagues utilized frozen tissue sections for their analysis (7), although it was noted in a comparison subset of paraffin-embedded samples assessed that there were no differences in END measures in frozen versus paraffin-embedded samples. Although these comparisons suggest that it may be challenging to compare END across studies, END measures seem to have potential when compared on a relative scale across studies, which is supported by findings in this analysis that showed strong relationships between END and TDLUs/localized MD when tertiles of each measure were examined.

BBD severity is related to increased breast cancer risk, but individual risk stratification remains a challenge. Previous reports (4, 15) demonstrate that levels of TDLU involution in background normal breast tissue are an important modifier of breast cancer risk, suggesting that methods for assessing normal structures contained within BBD biopsies may have utility. In this study, TDLUs were assessed visually in background normal tissues, whereas the END algorithm did not discriminate between normal and BBD on the whole slide image. Thus, although automated assessments of END by image analysis were associated with TDLU density assessed visually, particularly in nonproliferative BBD biopsies, measures of TDLUs and END were not perfectly correlated. Likewise, associations between END and MD measures also tended to be stronger in the setting of nonproliferative BBD. Therefore, these findings support that END and TDLU metrics may be complementary and suggest that END may not be an ideal surrogate method for assessment of TDLU involution, especially within the setting of BBD. Our *post hoc* sensitivity analysis supports this observation as we observed that specific annotated measures of segmented END, restricted to the background normal tissue on the slide showed stronger associations with TDLU counts than the agnostic quantification of END completed by the GENIE algorithm on the whole slide image. Thus, although the END algorithm may be useful in quantifying the number of epithelial nuclei, it may be unreliable in the setting of BBD. Additional limitations within this study include the relatively small sample size, particularly for analyses stratified by BBD diagnosis. Furthermore, as the current study population is composed of mostly white women, the generalizability of the study findings is limited and additional studies are needed to examine histologic measures of breast tissue epithelial composition across diverse populations. Give the large number of statistical tests carried out, the findings observed may also be due to chance and this must be acknowledged during the interpretation of the study analysis.

As improvements in automated digital pathology approaches continue, the information that can be gained and lost through such approaches must be recognized. For example, the END algorithm used in this study was not trained to differentiate immune cells from epithelial nuclei; as such, a small number of lymphocytes in intralobular connective tissue was included in END calculations. Although a pathologist would be able to discriminate between these two cell types, manual END enumeration would be time-intensive. In the future, use of more specialized algorithms, including the development and application of computational methods, may provide more precise END measurement. This interdisciplinary study used traditional and novel pathologic and radiological approaches and provides further evidence of the heterogeneous nature of BBD lesions. Future applications of digital pathology to diagnostic breast biopsies may provide opportunities to extend our understanding of breast cancer risk among women with BBD and the underpinnings of specific risk factors, such as MD.

Disclosure of Potential Conflicts of Interest

No potential conflicts of interest were disclosed.

Authors' Contributions

Conception and design: M. Mullooly, M.E. Sherman, M.A. Troester, G.L. Gierach

Development of methodology: M. Mullooly, S. Malkov, J.M. Johnson, S.M. Hewitt, M.E. Sherman, M.A. Troester, E.L. Kirk, R.M. Pfeiffer, L.T. Olsson, G.L. Gierach

Acquisition of data (provided animals, acquired and managed patients, provided facilities, etc.): E.L. Kirk, P.M. Vacek, D.L. Weaver, J. Shepherd, A. Mahmoudzadeh, J. Wang, S. Malkov, J.M. Johnson, S.M. Hewitt, S.D. Herschorn, M.E. Sherman, M.A. Troester, G.L. Gierach, L.T. Olsson, S. Puvanesarajah

Analysis and interpretation of data (e.g., statistical analysis, biostatistics, computational analysis): M. Mullooly, S. Puvanesarajah, S. Fan, R.M. Pfeiffer, L.T. Olsson, M. Hada, D.L. Weaver, A. Mahmoudzadeh, J. Wang, S. Malkov, J.M. Johnson, M.E. Sherman, G.L. Gierach

Writing, review, and/or revision of the manuscript: M. Mullooly, S. Puvanesarajah, S. Fan, R.M. Pfeiffer, M. Hada, P.M. Vacek, D.L. Weaver, J. Shepherd, J. Wang, J.M. Johnson, S.M. Hewitt, S.D. Herschorn, M.E. Sherman, M.A. Troester, G.L. Gierach

Administrative, technical, or material support (i.e., reporting or organizing data, constructing databases): M. Mullooly, S. Fan, L.T. Olsson, E.L. Kirk, D.L. Weaver, J.M. Johnson

Study supervision: G.L. Gierach, M.E. Sherman, M.A. Troester

Acknowledgments

The authors are indebted to all the women who generously participated in the BREAST-Stamp Project. The authors are also indebted to the efforts of the physicians, pathologists, nurses, technologists, and interviewers who contributed to this study. The authors thank past research coordinators at The University of Vermont, Claire Bove, Rachael Chicoine, and Patricia Lutton. The authors are grateful to Janet Lawler-Heaver and Kerry Grace Morrissey from Westat for the study management support and Jane Demuth at Information Management Services for data support and analysis. This study was supported by the Intramural Research Program of the NCI at the NIH. This research was also funded in part by the Health Research Board in Ireland (CPFPR-2013-1). This work was also supported by the Avon Foundation, North Carolina University Cancer Research

Fund, NCI (R01 CA179715), and National Institutes of Environmental Health Sciences U01 ES019472.

The costs of publication of this article were defrayed in part by the payment of page charges. This article must therefore be hereby marked *advertisement* in accordance with 18 U.S.C. Section 1734 solely to indicate this fact.

Received February 27, 2019; revised September 9, 2019; accepted October 17, 2019; published first October 23, 2019.

References

1. Boyd NF, Lockwood GA, Byng JW, Tritchler DL, Yaffe MJ. Mammographic densities and breast cancer risk.Cancer Epidemiol Biomarkers Prev 1998;7:1133–44.
2. McCormack VA, dos Santos Silva I. Breast density and parenchymal patterns as markers of breast cancer risk: a meta-analysis. Cancer Epidemiol Biomarkers Prev 2006;15:1159–69.
3. Russo J, Hu YF, Yang X, Russo IH. Developmental, cellular, and molecular basis of human breast cancer.J Natl Cancer Inst Monogr 2000:17–37.
4. Ghosh K, Vachon CM, Pankratz VS, Vierkant RA, Anderson SS, Brandt KR, et al. Independent association of lobular involution and mammographic breast density with breast cancer risk.J Natl Cancer Inst 2010;102:1716–23.
5. Gandomkar Z, Brennan PC, Mello-Thoms C. Computer-based image analysis in breast pathology.J Pathol Inform 2016;7:43.
6. Figueroa JD, Pfeiffer RM, Brinton LA, Palakal MM, Degnim AC, Radisky D, et al. Standardized measures of lobular involution and subsequent breast cancer risk among women with benign breast disease: a nested case-control study.Breast Cancer Res Treat 2016;159:163–72.
7. Sandhu R, Chollet-Hinton L, Kirk EL, Midkiff B, Troester MA. Digital histologic analysis reveals morphometric patterns of age-related involution in breast epithelium and stroma.Hum Pathol 2016;48:60–8.
8. Chollet-Hinton L, Puvanesarajah S, Sandhu R, Kirk EL, Midkiff BR, Ghosh K, et al. Stroma modifies relationships between risk factor exposure and age-related epithelial involution in benign breast.Mod Pathol 2018;31:1085–96.
9. Felix AS, Lenz P, Pfeiffer RM, Hewitt SM, Morris J, Patel DA, et al. Relationships between mammographic density, tissue microvessel density, and breast biopsy diagnosis.Breast Cancer Res 2016;18:88.
10. Gierach GL, Geller BM, Shepherd JA, Patel DA, Vacek PM, Weaver DL, et al. Comparison of mammographic density assessed as volumes and areas among women undergoing diagnostic image-guided breast biopsy.Cancer Epidemiol Biomarkers Prev 2014; 23:2338–48.
11. Gierach GL, Patel DA, Pfeiffer RM, Figueroa JD, Linville L, Papathomas D, et al. Relationship of terminal duct lobular unit involution of the breast with area and volume mammographic densities.Cancer Prev Res 2016;9:149–58.
12. Khodr ZG, Sherman ME, Pfeiffer RM, Gierach GL, Brinton LA, Falk RT, et al. Circulating sex hormones and terminal duct lobular unit involution of the normal breast.Cancer Epidemiol Biomarkers Prev 2014;23:2765–73.
13. Rosebrock A, Caban JJ, Figueroa J, Gierach G, Linville L, Hewitt S, et al. Quantitative analysis of TDLUs using adaptive morphological shape techniques.Proc SPIE Int Soc Opt Eng 2013;8676.
14. Liang K-Y, Zeger SL. Longitudinal data analysis using generalized linear models.Biometrika 1986;73:13–22.
15. Ghosh K, Hartmann LC, Reynolds C, Visscher DW, Brandt KR, Vierkant RA, et al. Association between mammographic density and age-related lobular involution of the breast.J Clin Oncol 2010;28:2207–12.